J. Fluid Mech. (1967), *vol.* 27, *part* 2, *pp.* 253–272
Printed in Great Britain

Stability of turbulent channel flow, with application to Malkus's theory

By W. C. REYNOLDS
Department of Mechanical Engineering, Stanford University, Stanford, California
AND W. G. TIEDERMAN
Shell Development Company, Emeryville, California

(Received 28 March 1966)

The Orr–Sommerfeld stability problem has been studied for velocity profiles appropriate to turbulent channel flow. The intent was to provide an evaluation of Malkus's theory that the flow assumes a state of maximum dissipation, subject to certain constraints, one of which is that the mean velocity profile is marginally stable. Dissipation rates and neutral stability curves were obtained for a representative two-parameter family of velocity profiles. Those in agreement with experimental profiles were found to be stable; the marginally stable profile of greatest dissipation was not in good agreement with experiments. An explanation for the apparent success of Malkus's theory is offered.

1. Introduction

The steady, fully developed flow of an incompressible Newtonian fluid between two stationary infinite parallel planes is known as plane Poiseuille flow. Although the parabolic velocity profile of laminar Poiseuille flow is well known, the corresponding theory for turbulent flow is not yet satisfactory. The major difference between the two cases is the existence of finite velocity fluctuations in turbulent flow. The interaction of these fluctuations yields a mean non-linear momentum transport (the 'Reynolds stress'). This transport gives rise to an additional unknown in the mean momentum equations, and since methods for calculating this unknown are not available the problem is not closed.

At the present time, the sole purely theoretical prediction of the mean velocity profile is that of Malkus (1956). Malkus completes the closure with a variational postulate; he assumes that the rate of energy dissipation is a maximum, and that the mean and fluctuating fields satisfy certain constraints. As he states them, two of these constraints are: 'First, that the mean flow will be statistically stable if an Orr–Sommerfeld type equation is satisfied by fluctuations of the mean; second, that the smallest scale of motion that can be present in the spectrum of the momentum transport is the scale of the marginally stable fluctuations of the mean.' Thus, he restricts the admissible class of velocity profiles to those which have a marginally stable fluctuation and which are determined by a Reynolds stress composed of fluctuations no smaller than the indicated smallest scale. As will be discussed later, these restrictions imply that the mean velocity profile is marginally stable in the Orr–Sommerfeld sense. He then proposes to select from

this class that profile which renders the rate of energy dissipation a maximum. The actual solution was obtained by an inversion of this maximization procedure, and numerous approximations were involved. Nevertheless, it is striking that the mean velocity profile that he calculated in this purely theoretical manner closely resembles the profile measured by Laufer (1951).

Malkus introduces the Orr–Sommerfeld problem into his theory by examining a perturbation of the mean velocity field, along the lines of classical stability theory (cf. Lin 1955). He assumes that the interaction of these small-amplitude velocity and pressure disturbances with the existing field of finite fluctuations

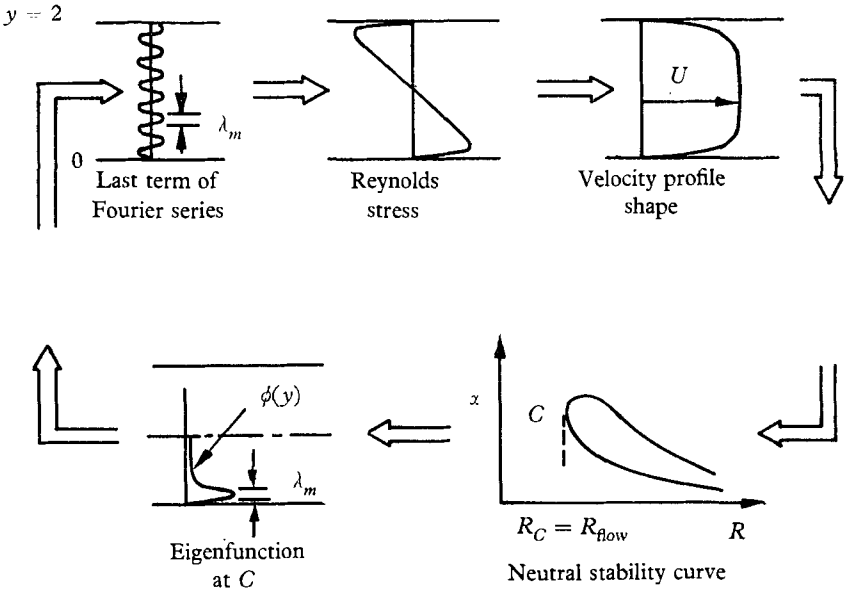

FIGURE 1. Conceptual scheme of Malkus's theory.

(the 'background turbulence') is stabilizing. When terms which represent this interaction are omitted from the first-order perturbation equation, the Orr–Sommerfeld problem (with the turbulent mean velocity profile) results. It is this problem which is used to restrict the admissible family of mean velocity profiles.

The family of admissible profiles is developed by expanding the Reynolds stress† in a finite series of periodic functions of y, chosen such that each term has more oscillations (in y) than the preceding term. The oscillation of the last member of the series sets the *smallest scale* of oscillation, or smallest wave length λ_m. This presumably represents the smallest scale of motion present in the turbulence, and is extremely important in the Malkus theory.

The Orr–Sommerfeld problem plays a key role in Malkus's estimate of λ_m. These conditions upon the last term of the series may be visualized as in figure 1.

† This simplification accurately reflects the conceptual idea. Actually a function d^2 was expanded, where

$$\text{Reynolds stress} \sim \int_1^y (d^2 - 1)\, dy.$$

This allowed Malkus to guard against admitting profiles which would have inflexion points, which inherently lead to dynamic instability.

The Reynolds stresses are determined from the series summation where the last term has a scale λ_m. From the Reynolds stress a velocity profile shape is determined; and from the Orr–Sommerfeld equation, the neutral stability curve for this profile shape is obtained. The eigenfunction corresponding to $R_{\text{crit.}}$ is then determined and the scale of its fluctuation is required to be compatible with λ_m. Moreover, $R_{\text{crit.}}$ is required to emerge finally as the flow Reynolds number, so that the mean profile is marginally stable. These constraints determine the class of profiles which is admissible in the extremizing process.

We propose to make the following test of these ideas. For some selected Reynolds number, we shall take the known mean velocity profile *shape*, and calculate the corresponding neutral stability curve, considering R to be a variable. The test will be successful if the critical Reynolds number determined from this curve matches the flow Reynolds number, as shown in figure 2.

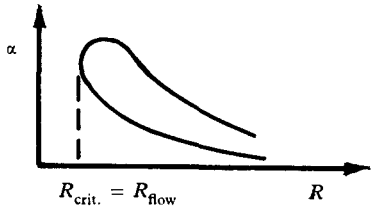

FIGURE 2. The idea of a marginally stable mean velocity profile.

There has been considerable conjecture about the role of the Orr–Sommerfeld problem in Malkus's theory. Townsend (1962) rephrases the constraint as 'marginal stability of the last member of the series' (in the expansion of the Reynolds stress). He further states that 'the modes of motion considered by Malkus are motions obtaining energy directly from the mean flow and losing it by non-linear transfer...'. These rephrasings suggest an expansion in terms of *unstable* eigenfunctions of the linear problem. In subsequent commentary Spiegel (1962) appeared to have the same view. He presumed that at each value of α and R a number of eigenvalues and their associated normal-mode eigenfunctions exist as solutions to the Orr–Sommerfeld problem. Spiegel conjectured that each of these normal modes has a neutral stability curve somewhere in the (α, R)-plane, as shown in figure 3. The dashed line indicates Spiegel's interpretation of the flow Reynolds number. Since higher mode neutral stability curves had not been calculated for any shear flow, Spiegel suggested their position and shape from the analogous neutral stability modes of thermal convection. He then suggested that the last member in the finite series should be determined from the $n = n^*$ mode. Landahl (1965) stated that Malkus 'hypothesized that the velocity fluctuations must be selected within that class of marginally stable fluctuations...', which again suggests a representation of the turbulence in terms of the neutrally stable eigenmodes. Lumley (1966) appears to have held a similar view. There is no evidence that a family of neutral stability curves exists for shear flows. In fact all numerical calculations for laminar Poiseuille flow indicate that there is only one unstable mode and hence only one neutral curve (Howard 1964; Lee & Reynolds 1964). These interpretations appear to be inconsistent with

Malkus's stated objective 'to find the momentum transport spectrum and mean velocity profile which lead to a marginally stable mean field of maximum dissipation rate'.

There are other difficulties with Malkus's theory. Spiegel pointed out that there is no assurance that the proposed optimum state is allowed by the equations of motion. Moreover, it is not apparent that the extremum problem Malkus actually solved can be properly inverted to the initial variational postulate of maximum dissipation rate at a fixed Reynolds number. There is also no thermodynamic reason for expecting the dissipation to be a maximum under these, or any other, constraints.†

The objective of the present study was to evaluate all of these ideas. The method of attack centred on a direct calculation of dissipation and the determination of the neutral stability curves for a family of turbulent plane Poiseuille profiles. The family of profiles was calculated from the mean equations of motion

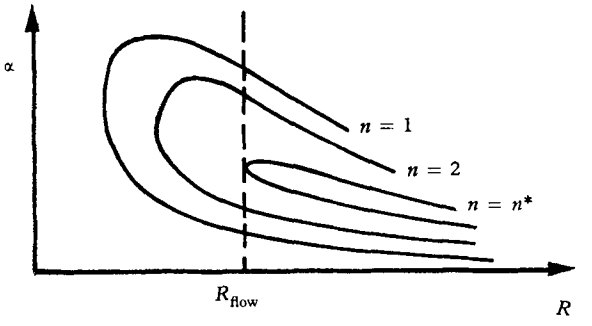

FIGURE 3. Spiegel's interpretation of Malkus's theory.

after the Reynolds stresses were determined from an assumed expression for eddy viscosity. This expression, and hence the mean profile, contains two free parameters. The dissipation rate and the neutral stability curves were determined as functions of these two parameters for a fixed flow Reynolds number, and in particular for marginally stable members of the two parameter family. Based on these calculations, we can draw some conclusions relative to the important aspects of Malkus's theory, and these are given in §4.

2. Characteristics of the mean velocity field

The equations relating the mean velocity profile to the turbulent Reynolds stress are obtained by representing the velocity field by the sum of a mean and a fluctuation, and averaging. When suitably normalized, they become (see figure 4)

$$\frac{d}{dy}(\overline{uv}) = -\frac{\partial P}{\partial x} + \frac{1}{R}\frac{d^2U}{dy^2}, \tag{2.1a}$$

$$\frac{d\overline{v^2}}{dy} = -\frac{\partial P}{\partial y}. \tag{2.1b}$$

† See the discussion by one of us on the paper by Sparrow & Siegel (1959).

Here the channel half width, δ, is used as the characteristic length, and the continuity-average velocity, U_m, is used to normalize both the fluctuating velocities u and v and the mean field U. U_m is defined by the condition that

$$\int_0^1 U(y_1)\,dy_1 = 1. \tag{2.2}$$

The mean pressure P is normalized on ρU_m^2, and the Reynolds number is

$$R = U_m\delta/\nu,$$

where ν is the kinematic viscosity. If a scalar eddy viscosity is used instead of the Reynolds stress, (2.1a) becomes

$$\frac{\partial P}{\partial x} = \frac{1}{R}\frac{d}{dy}\left[(1+E)\frac{dU}{dy}\right]. \tag{2.1c}$$

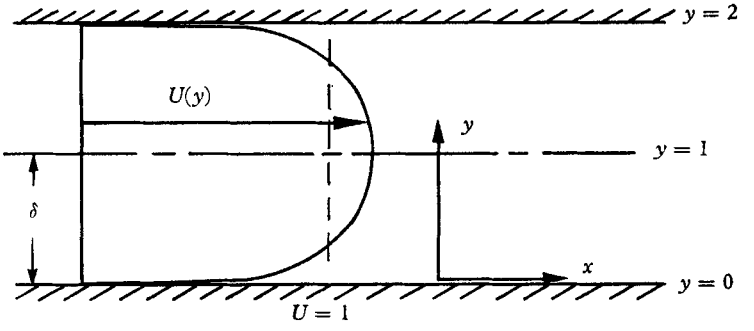

FIGURE 4. Co-ordinates for the channel flow.

Here E is the (kinematic) eddy viscosity, normalized on ν, and defined by comparison of (2.1a) and (2.1c).

Equation (2.1b) indicates that the streamwise pressure gradient is uniform across the flow, and hence may be replaced by the wall pressure gradient, $dP_w/dx = -B$. Then, (2.1c) may be integrated twice, employing the conditions that $U(0) = 0$, and $U'(1) = 0$,† and the mean velocity field is obtained as

$$U(y) = RB\int_0^y \frac{1-y_1}{1+E(y_1)}\,dy_1. \tag{2.3}$$

The value of the streamwise pressure gradient is fixed by (2.2). Thus, given the eddy viscosity distribution, the mean velocity profile can be evaluated using appropriate numerical techniques.

The mean dissipation rate per unit of length may be determined by considering the control volume of figure 5. If one assumes that the fluid is incompressible [and hence the internal energy and entropy are functions of temperature only (Reynolds 1965)], and that conduction mechanisms maintain an isothermal flow, then application of the second law of thermodynamics gives the rate of entropy production per unit of length as

$$\dot{P}_s = q/T. \tag{2.4}$$

† Primes denote differentiation.

Here q is the rate at which energy is transferred as heat from the control volume (per unit length), and T is the fluid temperature. Note that the convective entropy fluxes cancel for steady, fully developed isothermal flow. An energy balance on the control volume, incorporating these idealizations, yields (unnormalized)

$$q+\rho U_m^3\int_0^{2\delta}\frac{\partial P}{\partial x}U\,dy=0. \tag{2.5}$$

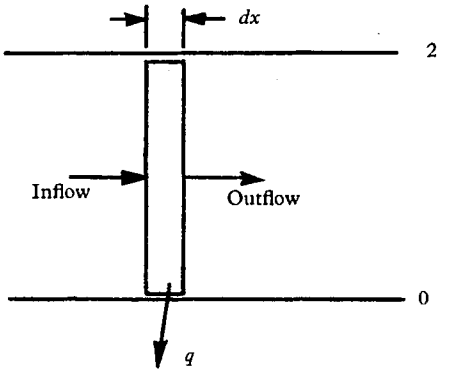

FIGURE 5. Control volume.

Using (2.4), the (normalized) rate of entropy production is

$$\mathscr{D}=T\dot{P}_s/(\rho U_m^3)=2B. \tag{2.6}$$

This is consistent with the dissipation expression used by Malkus.

It is important to appreciate that the laws of thermodynamics state that the entropy of an isolated system must increase, but say nothing about the *rate* of entropy production. In fact, it is known that a principle of minimum (or maximum) dissipation rate does not in general hold (Gage *et al.* 1966), and consequently Malkus's use of such a principle was purely speculative.

The expression for eddy viscosity which we used was first suggested by Cess (1958) for pipe flow. It has the advantage of being continuous and analytic, and this allowed complex continuation in our asymptotic treatment of the stability problem. The expression is a combination of van Driest's wall region law and Reichardt's middle law, and, as adapted for the channel, is

$$E(y)=\tfrac{1}{2}\left\{1+\frac{K^2R^2B}{9}[2y-y^2]^2[3-4y+2y^2]^2\left[1-\exp\left(\frac{-yR\sqrt{B}}{A^+}\right)\right]^2\right\}^{\frac{1}{2}}-\tfrac{1}{2}. \tag{2.7}$$

The constant K is the von Kármán constant of the logarithmic velocity profile, and A^+ is a constant in van Driest's wall law, characterizing the thickness of the wall region in the shear velocity normalized (y^+) co-ordinate. A^+ and K are the two parameters used to characterize the profiles throughout this study.

The nominal values of K and A^+ which fit experiments in pipe flow are 0·4 and 26, respectively. Values of 0·4 and 31 give a somewhat better fit to the channel flow data of Laufer (1951). The mean profile for these latter values is plotted in the usual shear-velocity normalized co-ordinates in figure 6. Profiles for other

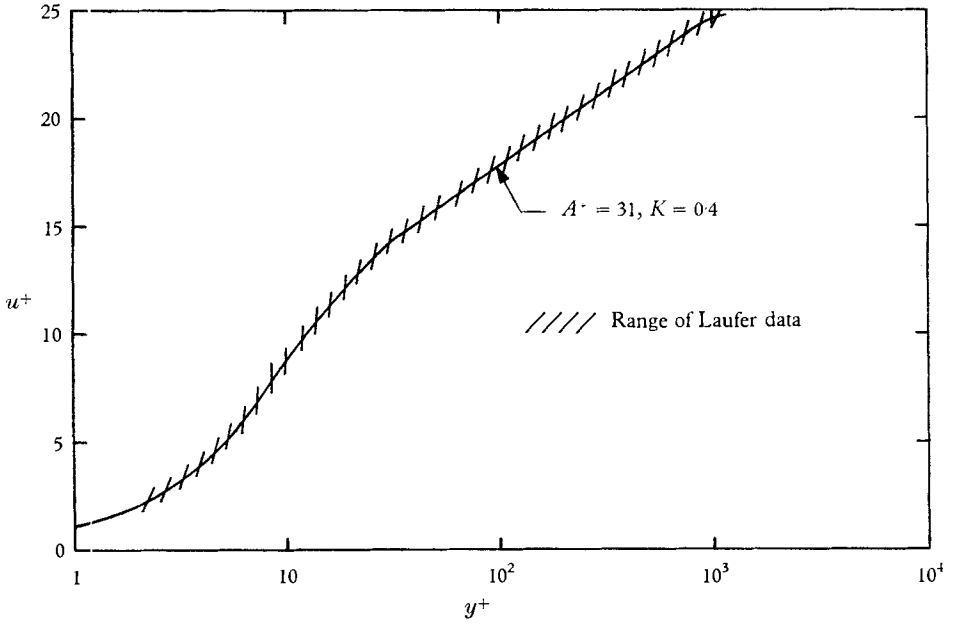

FIGURE 6. Comparison of the analytical profile with Laufer's experiments.

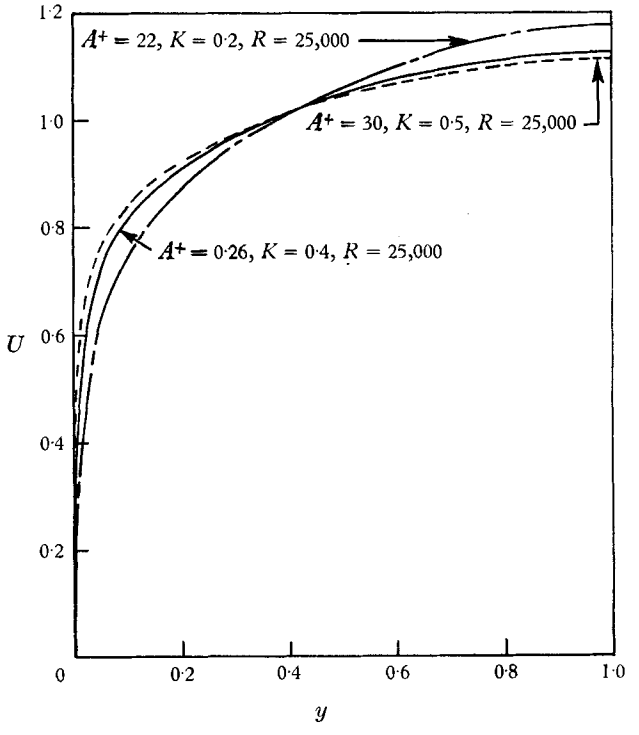

FIGURE 7. Members of the admissible family.

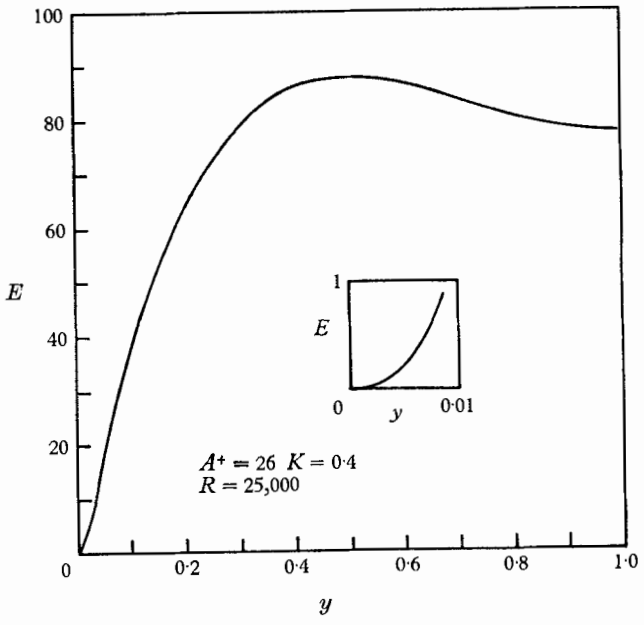

FIGURE 8. Eddy viscosity on the real axis.

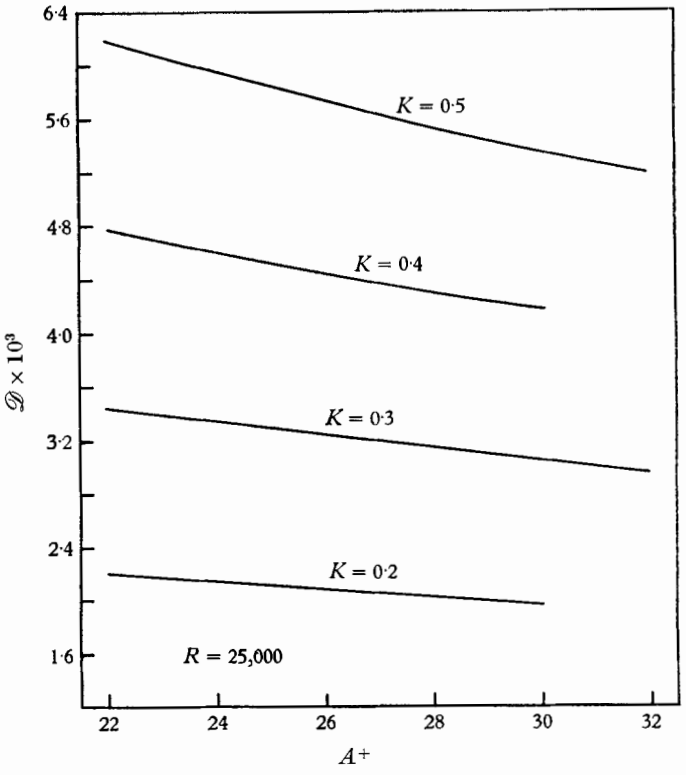

FIGURE 9. Dissipation for some members of the admissible family.

values of the parameters are shown in figure 7 for comparison. The eddy viscosity for a typical case is shown in figure 8.

The dissipation rate $\mathscr{D}$ was calculated for a number of combinations of the parameters, and the results are shown in figure 9. Note that no apparent minimum or maximum appears, and it is consequently clear that a hypothesis of minimum or maximum dissipation without constraints would be invalid.

Malkus actually solved an inverted extremum problem; fixing the product of the friction factor and Reynolds number, i.e. RB, he sought the flow of minimum Reynolds number. He implied that this was equivalent to minimizing the flow at fixed dissipation, but this would not appear to be the case. The values of Reynolds number corresponding to fixed values of RB were calculated, and again no unconstrained extremum was evident.

It is clear from these simple calculations that the constraints of Malkus's theory are essential. The Orr–Sommerfeld problem for the turbulent velocity profile plays a key role in constraints, and Malkus used a very simplified stability treatment. Since the eigenvalues of the Orr–Sommerfeld equation are very sensitive to the shape of the profile, we felt it would be highly desirable to carry out a more exact stability analysis, and this work is described in the next section.

3. Solution of the Orr–Sommerfeld problem

Investigations of the stability of parallel flows involve the Orr–Sommerfeld equation, which results from introducing specific forms of the small amplitude velocity and pressure perturbations into the Navier–Stokes equations. If the same procedure is followed in turbulent flow, additional terms are obtained; these reflect the interaction of the infinitesimal perturbation wave with the background turbulence of finite fluctuation. Malkus took the view that the interaction between the finite fluctuations and the perturbation would tend to stabilize the perturbation, and hence from the point of view of wanting to reject *unstable* turbulent profiles it would be conservative to neglect this complex interaction. Consequently he worked with the same Orr–Sommerfeld equation as emerges in analysis of laminar instability, but imagined using mean velocity profiles appropriate for turbulent flow.

It is known that the stability of parallel viscous flows to oblique wave disturbances can be studied by considering only waves which travel in the streamwise direction. Since the lowest Reynolds number at which an instability will occur corresponds to a wave aligned with the flow direction (cf. Lin 1955), it is enough to study such disturbances.

Introducing a streamwise wave having a streamfunction of the form

$$\psi(x,y,t) = \phi(y)\exp[i\alpha(x-ct)] \tag{3.1}$$

into the equations of motion, and neglecting (as did Malkus) any interaction between the infinitesimal wave and the background turbulence, one obtains the (normalized) Orr–Sommerfeld equation for the wave amplitude distribution, $\phi(y)$,

$$\phi^{\mathrm{iv}} - 2\alpha^2\phi'' + \alpha^4\phi = i\alpha R[(U-c)(\phi''-\alpha^2\phi) - U''\phi]. \tag{3.2a}$$

The boundary conditions at the walls give

$$\phi(0) = \phi'(0) = \phi(2) = \phi'(2) = 0. \tag{3.2b}$$

Here primes denote differentiation, $U(y)$ is the parallel basic flow under study, α is the wave-number, and $c = c_r + ic_i$ is the eigenvalue associated with the eigenfunction $\phi(y)$. The wave speed is c_r, and c_i determines whether the wave amplitude will grow ($c_i > 0$) or decay ($c_i < 0$) in time. The curve in the (α, R)-plane along which $c_i = 0$ is called the neutral (marginal) stability curve, and it separates regions of stable and unstable response to the wave disturbance.

The velocity profile must be specified before the Orr–Sommerfeld problem can be solved, and in the present case we wish to do this for profile shapes appropriate to turbulent channel flow. These shapes are actually dependent upon the flow Reynolds number, R_{flow}; we will use the normalized profiles calculated as described previously for a particular R_{flow} in the Orr–Sommerfeld solutions, allowing R to vary in the Orr–Sommerfeld problem. The solutions of interest will then be points where $R = R_{\text{flow}}$.

The velocity profiles for channel flow are all symmetric about the centreline, and the operators in the Orr–Sommerfeld equation are all even; consequently the eigenfunctions will either be symmetric or antisymmetric, and this fact can be used to reduce the range of solution to $0 \leqslant y \leqslant 1$. The boundary conditions then become

$$\phi(0) = \phi'(0) = \phi'(1) = \phi'''(1) = 0 \quad \text{for symmetric eigenfunctions} \tag{3.3}$$

and

$$\phi(0) = \phi'(0) = \phi(1) = \phi''(1) = 0 \quad \text{for antisymmetric eigenfunctions.} \tag{3.4}$$

The general solution may be written as the sum of four linearly independent solutions of (3.2a),

$$\phi = C_1\phi_1 + C_2\phi_2 + C_3\phi_3 + C_4\phi_4. \tag{3.5}$$

Imposition of the boundary conditions leads to a set of four simultaneous homogeneous linear equations for the constants $C_1 \ldots C_4$, which can only possess non-trivial solutions if the determinant of the matrix vanishes. This requirement produces the condition from which the eigenvalues c are determined. Denoting $\phi_{j1} = \phi_j(0)$ and $\phi_{j2} = \phi_j(1)$, the secular equation is, for symmetric eigenfunctions,

$$F_s(\alpha, c, R) = \begin{vmatrix} \phi_{11} & \phi_{21} & \phi_{31} & \phi_{41} \\ \phi'_{11} & \phi'_{21} & \phi'_{31} & \phi'_{41} \\ \phi'_{12} & \phi'_{22} & \phi'_{32} & \phi'_{42} \\ \phi'''_{12} & \phi'''_{22} & \phi'''_{32} & \phi'''_{42} \end{vmatrix} = 0 \tag{3.6}$$

and, for antisymmetric eigenfunctions,

$$F_a(\alpha, c, R) = \begin{vmatrix} \phi_{11} & \phi_{21} & \phi_{31} & \phi_{41} \\ \phi'_{11} & \phi'_{21} & \phi'_{31} & \phi'_{41} \\ \phi_{12} & \phi_{22} & \phi_{32} & \phi_{42} \\ \phi''_{12} & \phi''_{22} & \phi''_{32} & \phi''_{42} \end{vmatrix} = 0. \tag{3.7}$$

Four linearly independent solutions of the Orr–Sommerfeld equation are needed next. Since R is expected to be large, asymptotic methods have been found effective. Following Lin (1955), we seek solutions in the form†

$$\phi(y) = \phi^{(0)}(y) + (1/\alpha R)\,\phi^{(1)}(y) + \ldots. \tag{3.8}$$

Substituting, and considering the terms of lowest order, one finds

$$[(U-c)(D^2-\alpha^2) - U'']\,\phi^{(0)} = 0, \tag{3.9}$$

where $D = d/dy$. This term contains no information from the fourth-order viscous terms, and hence is called the 'inviscid' Orr–Sommerfeld equation. Since it is of second order, only two independent solutions can be obtained via the expansion (3.8). If α is not too large, these may be developed as power series in α^2; this is satisfactory for laminar plane Poiseuille flow (Lin 1955), but the values of interest in the present problem are sufficiently large that other methods must be used.‡ The two independent solutions ϕ_1 and ϕ_2 thereby obtained are called the 'inviscid' solutions, because they are, to first order, solutions of the inviscid equation. The higher-order approximations to ϕ_1 and ϕ_2 are not usually employed in the large Reynolds number range of common interest.

The solution of the inviscid equation must be carried out along an appropriately chosen path in the complex y-plane. The choice of path is dictated by the desire to render these two solutions valid asymptotic expansions of two solutions of the full Orr–Sommerfeld equation. Lin (1955) has shown that the proper choice is a path which lies *below* the point $U = c$ for $0 \leqslant y \leqslant 1$, the range of the present integrations. Hence, since for neutral stability we are interested in real c, it will be necessary to go off the real axis, circumventing the points where $U = c$ in the lower half-plane; this will require an analytic continuation of the velocity profile, which in turn requires a continuable expression for the eddy viscosity. It was with this in mind that the Cess expression was chosen.

Two additional solutions are needed, and these must incorporate information from the viscous terms. This requires a 'stretching' of the independent variable prior to the expansion in powers of a small parameter. The stretching which retains the necessary information is (Lin 1955)

$$\eta = (y-y_c)(\alpha R)^{\frac{1}{3}}, \tag{3.10}$$

where $U(y_c) = c$. Then ϕ is expanded such that

$$\phi(\eta) = \chi^{(0)}(\eta) + O[(\alpha R)^{-\frac{1}{3}}] \tag{3.11}$$

and U is expanded about y_c. With this stretching expansion, the first-order problem yields

$$D^4\chi^{(0)} - iU_c'\eta D^2\chi^{(0)} = 0. \tag{3.12}$$

Of the four linearly independent solutions of (3.12), two can be formally

† Recent numerical solutions of the full Orr–Sommerfeld equation (by W.C.R.) support the validity of using the asymptotic solution method for turbulent profiles.

‡ In an earlier report (Tiederman & Reynolds 1965) we used the series solution method, which yields results in accord with the present calculations at sufficiently small α. The present calculations, valid over the entire range of α, supersede those of the report.

identified with the two 'inviscid' solutions ϕ_1 and ϕ_2; the other two solutions, ϕ_3 and ϕ_4 (the 'viscous' solutions), are, to first order (Lin 1955)

$$\phi_{3,4} \approx \chi^{(0)}_{3,4}(\eta) = \int_{\pm\infty}^{\eta} \left\{ \int_{\pm\infty}^{\eta_1} \eta_2^{\frac{1}{2}} H^{(1,2)}_{\frac{1}{3}} [\tfrac{2}{3}(iU_c'^{\frac{1}{3}}\eta_2)^{\frac{3}{2}}]\, d\eta_2 \right\} d\eta_1. \tag{3.13}$$

Here $H^{(1)}_{\frac{1}{3}}$ is the Hankel function of the first kind, of order $\frac{1}{3}$, and $H^{(2)}_{\frac{1}{3}}$ is the corresponding function of the second kind. The viscous solutions, in this approximation, are valid close to y_c, where the stretched variable η is around unity. Normally the wall is in the region where η is relatively small, and hence these solutions provide adequate approximations at the wall. However, at the channel centreline the solutions are not sufficiently accurate; one can go to higher order, or alternatively develop the viscous solutions in a different manner. Lin (1955) shows how the W.K.B. method can be used to obtain asymptotic expansions of the viscous solutions valid away from the critical point, and how these W.K.B. solutions connect with the critical layer solutions. The asymptotic 'outer' expansions of the viscous solutions corresponding to ϕ_3 and ϕ_4 are found to be

$$\phi_{3,4}(y) \sim (U-c)^{-\frac{5}{4}} \exp\left[\mp \int_{y_c}^{y} \{i\alpha R(U-c)\}^{\frac{1}{2}}\, dy_1 \right]. \tag{3.14}$$

Lin further establishes that the appropriate branch of the square root which match these solutions to the 'inner' solutions is the one which renders the real part of the root *positive*. Hence ϕ_3 will decay rapidly as y increases towards the centreline, while ϕ_4 will grow.

For large R the main contribution to ϕ at the centre comes from ϕ_1, ϕ_2 and ϕ_4. Since $\phi'''_{42} \gg \phi'_{42}$, the main effect of ϕ_4 will be to allow ϕ''' to vanish at the centre (for symmetric eigenfunctions), and the centreline conditions are approximately

$$C_1\phi'_{12} + C_2\phi'_{22} = 0, \tag{3.15a}$$

$$C_1\phi'''_{12} + C_2\phi'''_{22} + C_4\phi'''_{42} = 0. \tag{3.15b}$$

Hence the relative amounts of ϕ_1 and ϕ_2 in the solution are essentially controlled by (3.15a). At the wall ϕ_4 is very small, but ϕ_3 contributes, and hence the wall boundary conditions are approximately

$$C_1\phi_{11} + C_2\phi_{21} + C_3\phi_{31} = 0, \tag{3.15c}$$

$$C_1\phi'_{11} + C_2\phi'_{21} + C_3\phi'_{31} = 0. \tag{3.15d}$$

Since the relative amounts of ϕ_1 and ϕ_2 in the complete solution are determined by the lower-order centreline boundary condition (3.15a), it is convenient to construct a linear combination of ϕ_1 and ϕ_2 which satisfies this condition and then to use this modified inviscid solution in conjunction with the two viscous solutions ϕ_3 and ϕ_4. The higher-order centreline condition (3.15b) establishes the amount of ϕ_4 required, and then the wall conditions (3.15c,d) provide the characteristic equation. Thus, we define a modified inviscid solution by (for symmetric eigenfunctions)

$$\phi_i = \phi_1 - (\phi'_{12}/\phi'_{22})\,\phi_2 \tag{3.16}$$

and the approximate characteristic equation becomes

$$\phi_{31}/\phi'_{31} = \phi_{i1}/\phi'_{i1}. \tag{3.17}$$

Similar arguments for antisymmetric eigenfunctions, incorporating a modified inviscid solution which vanishes at the centreline, again give (3.17) as the characteristic equation.

The viscous term ϕ_{31}/ϕ'_{31} is taken from the asymptotic solution (3.13) as (Lin 1955)

$$\phi_{31}/\phi'_{31} = -y_c F(z), \tag{3.18}$$

where $z = (\alpha R U'_c)^{\frac{1}{3}} y_c$ and

$$F(z) = \frac{\int_{\infty}^{-z} \int_{\infty}^{\zeta_1} \zeta_2^{\frac{1}{2}} H_{\frac{1}{3}}^{(1)}[\frac{2}{3}(i\zeta_2)^{\frac{3}{2}}]\, d\zeta_2\, d\zeta_1}{-z \int_{\infty}^{-z} \zeta_1^{\frac{1}{2}} H_{\frac{1}{3}}^{(1)}[\frac{2}{3}(i\zeta_1)^{\frac{3}{2}}]\, d\zeta_1}. \tag{3.19}$$

The characteristic equation can be put into a form more convenient for solution by dividing (3.17) by y_c, which gives

$$F(z) = G(\alpha, c), \tag{3.20}$$

where $\phi_{i1}/\phi'_{i1} = -y_c G(\alpha, c)$. Further ease at solution is obtained if we introduce the definitions

$$\mathscr{F}(z) = 1/[1 - F(z)] \quad \text{and} \quad \mathscr{G}(\alpha, c) = 1/[1 - G(\alpha, c)],$$

and then rewrite the characteristic equation as

$$\mathscr{F}(z) = \mathscr{G}(\alpha, c). \tag{3.21}$$

Note that both F and $\mathscr{F}$ are independent of the velocity profile shape. Miles (1960) calculated and tabulated $\mathscr{F}(z)$ for real z over the range of interest; this suffices for determination of the neutral stability curve. The inviscid function $\mathscr{G}(\alpha, c)$ must be calculated for a specific profile shape and then the characteristic equation can be solved by some suitable means.

After some considerable exploration of various possibilities, we ultimately decided to determine the inviscid solution by direct numerical integration. The path along which the solution was obtained is shown in figure 10. The circular arc was subdivided into eight parts, and 40 steps were used in each part. The steps of adjacent parts differed by factors of two, with the finest mesh located at the wall. The solution was started at the centreline, with the appropriate central conditions, and carried to the wall, where $\mathscr{G}(\alpha, c)$ was then calculated. A four-point integration scheme was used; ϕ'' at three backward points and the unknown forward point was used to find a third-order polynomial, which was then integrated to get an expression for ϕ at the forward point in terms of ϕ'' at this point. The differential equation was then used to find ϕ'' at the forward point. For large α the solution goes locally like $\exp(-Q\alpha y)$, where Q is a constant related to the velocity field, and hence it was desirable to begin the calculation at some point midway across the channel. An extensive series of numerical experiments substantiated the validity of the various numerical schemes employed, and showed that the resulting values of $\mathscr{G}$ were accurate to at least four places. The calculations were programmed in FORTRAN IV, which provides for automatic complex arithmetic, and executed on an IBM 7090.

The solution of the inviscid equation in the complex plane requires an analytic continuation of the velocity profile, which in turn requires analytic continuation

of $E(y)$. Provided that we stay sufficiently close to the real axis, (2.7) can be so continued, and hence the corresponding complex velocity profile can be computed from (2.3). In figure 11 we show the complex eddy viscosity for a typical case, and in figure 12 the corresponding complex velocity profile is shown.

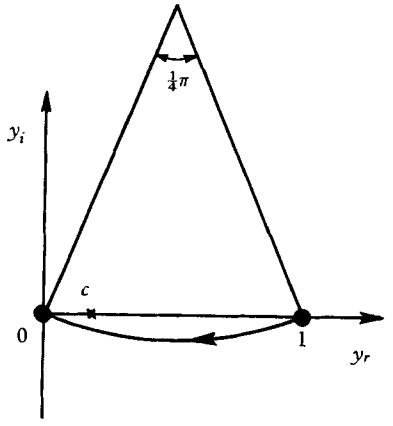

FIGURE 10. Path of integration for the inviscid solution.

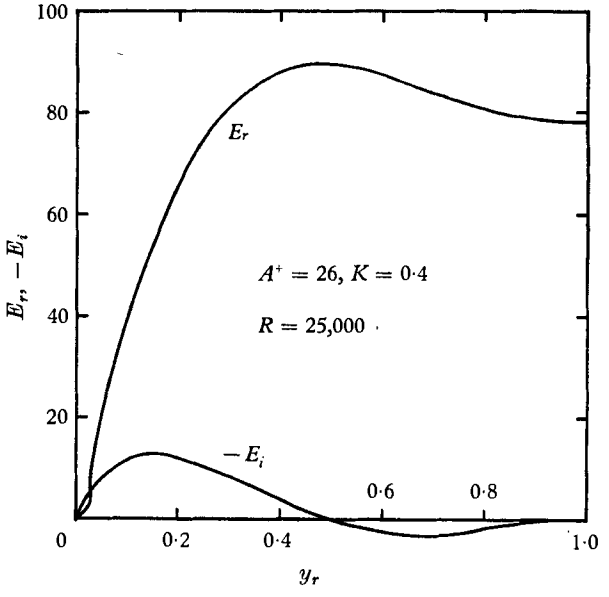

FIGURE 11. Eddy viscosity on the complex path.

Because $\mathscr{G}(\alpha, c)$ can be rapidly calculated, we find the eigenvalues for neutral stability using an Argand diagram (figure 13). The real and imaginary parts of $\mathscr{F}(z)$ are plotted from Miles's (1960) tabulation, and give the loop-like curve of figure 13. By solving the inviscid equation for a sequence of values of α at fixed c, and plotting the real and imaginary parts of $\mathscr{G}(\alpha, c)$ on the same graph, a line is obtained which, for sufficiently small c, intersects the $\mathscr{F}$ curve at two points, which therefore represent solutions to the characteristic equation (3.21). The

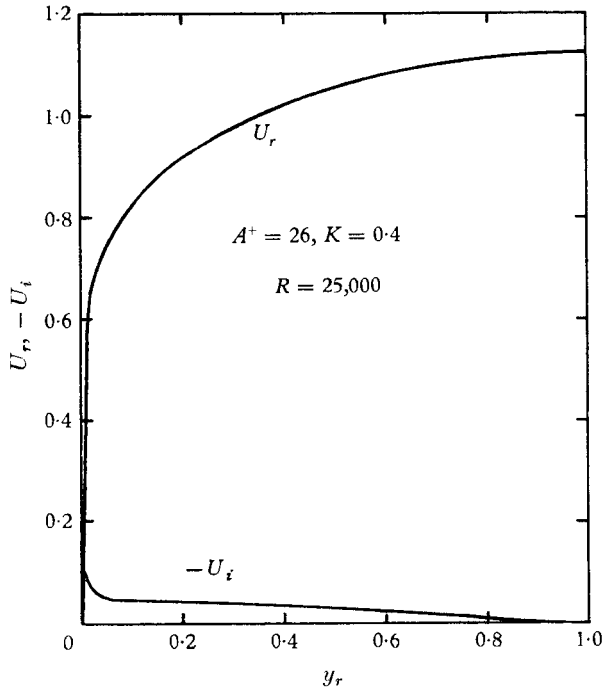

FIGURE 12. Velocity profile on the complex path.

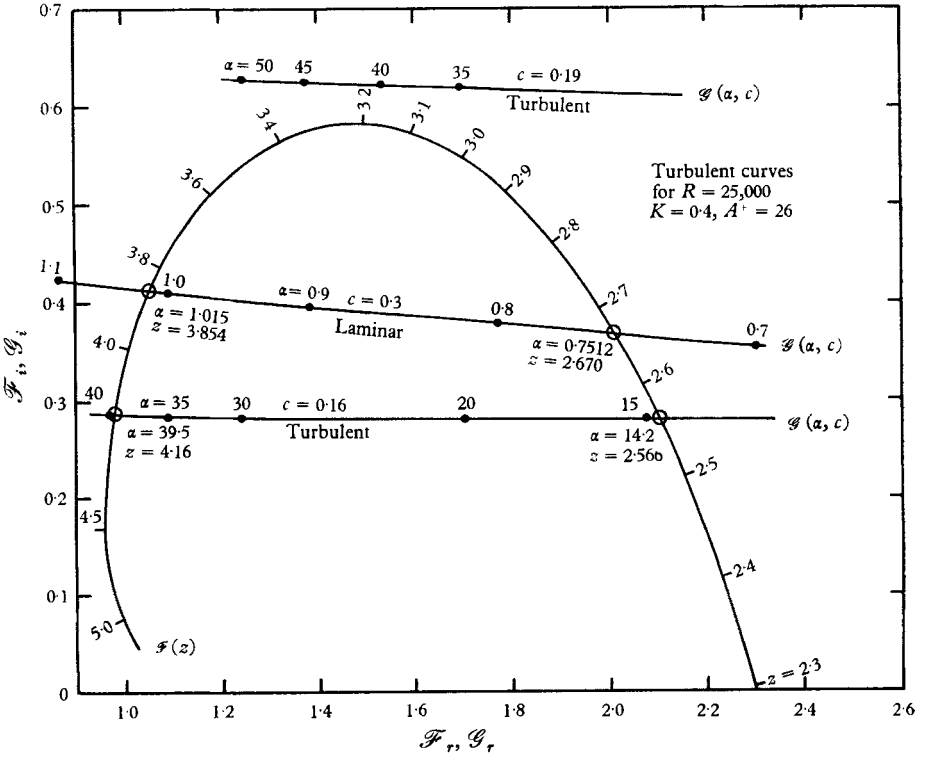

FIGURE 13. Argand diagram.

values of α and z at these intersections, together with c, determine R, with the dual intersections giving points on the two branches of the neutral stability curve. Two typical graphical solutions are shown in figure 13. The laminar solution, obtained using the present numerical programme, is in agreement with the results obtained earlier by Lin (1955). Note the large values of α which are of interest in the turbulent case. In an earlier attempt to study this problem (Tiederman & Reynolds 1965) we computed the inviscid solution as a series in α^2, using numerical integration of the integrals given by Lin. The values of $\mathscr{G}$ deduced subsequently from these earlier calculations are in excellent agreement with those of the present calculation for $\alpha < 2$, and the points on the neutral stability curves for $\alpha < 1$ found previously are again substantiated.† This check with the earlier, independent calculation, provides considerable confidence for the present calculations.

Observing that the Argand-diagram lines of constant c from the inviscid calculations are very nearly straight lines, an approximate scheme for calculating the critical Reynolds number is suggested. The two points of intersection on the Argand diagram will meet approximately at $z = 3{\cdot}2$, and hence the characteristic equation at the critical Reynolds number is approximately

$$\mathscr{G}(\alpha, c) = 1{\cdot}497 + 0{\cdot}581i, \tag{3.22a}$$

$$(\alpha R_{\text{crit.}} U_c')^{\frac{1}{3}} y_c = 3{\cdot}2. \tag{3.22b}$$

We used this as a basis for approximate calculation of $R_{\text{crit.}}$, and found it to be in good agreement with the graphical results.

The results of the stability study for turbulent profiles will now be described.

4. Results and discussion

Calculations for symmetric eigenfunctions for profiles closely resembling the experimental turbulent profiles of Laufer (1951) were carried out at a flow Reynolds number of 25,000. Two typical neutral stability curves for such profiles are shown in figure 14. Note that the critical Reynolds number for these profiles is a factor of 10 greater than the flow Reynolds number; the experimental profile is *not*, as Malkus supposed, marginally stable.‡

There is, however, a subset of profiles from our two-parameter family which are marginally stable, and some are shown in figure 15. Note that the values of A^+ and K corresponding to these profiles differ substantially from the 'experimental' values, as do the profiles themselves. The value of A^+ which, for a given K, yields a marginally stable profile is shown in figure 16. Note that, for large K and A^+, a limiting behaviour of $A^+/K = \text{const.}$ is obtained. The dissipation rate for these marginally stable profiles is also shown in figure 16. Note that it ap-

† In the previous work we used Lin's (1955) iteration method, rather than the Argand diagram, to solve the characteristic equation, and obtained neutral stability curves considerably different from those we report here. The failing of the earlier calculation was due to a very high sensitivity of the iterative scheme to the initialization. The earlier results should be disregarded for $\alpha > 1$.

‡ At the large values of α involved near the critical point, symmetric and antisymmetric eigenfunctions give indistinguishable eigenvalues.

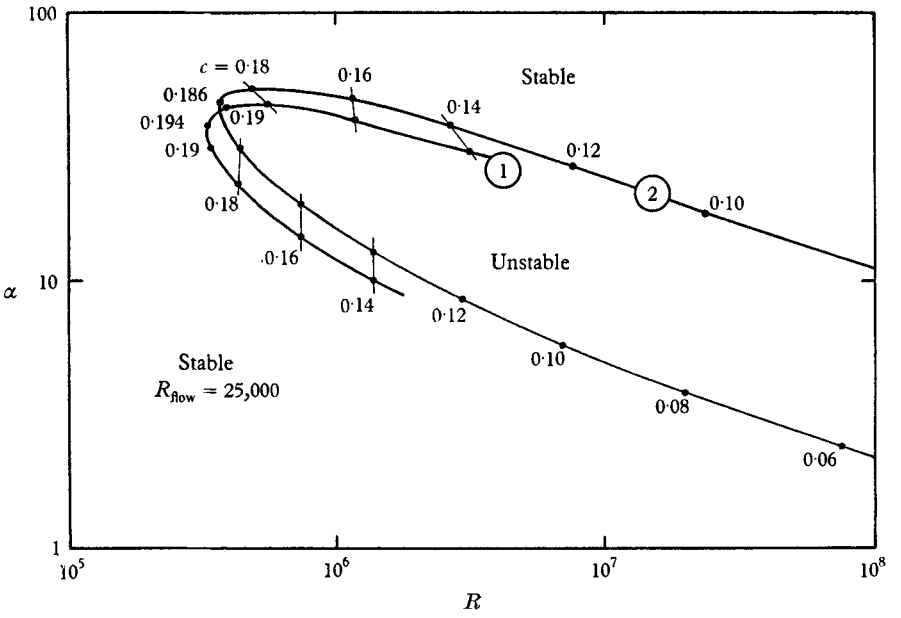

FIGURE 14. Neutral stability curves for turbulent profiles.
1, $K = 0{\cdot}4$, $A^+ = 31$; 2, $K = 0{\cdot}4$, $A^+ = 26$.

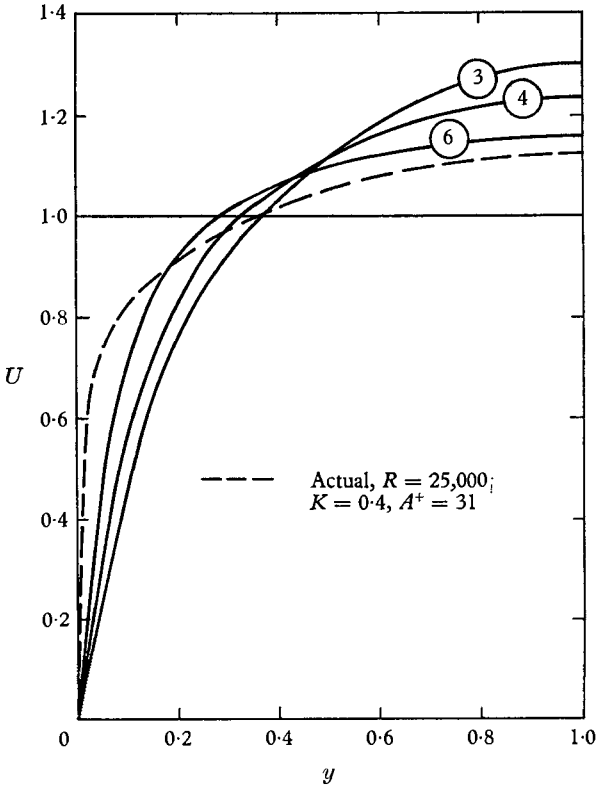

FIGURE 15. Neutrally stable members of the admissible family.
3, $K = 0{\cdot}05$, $A^+ = 78$; 4, $K = 0{\cdot}10$, $A^+ = 137$; 6, $K \to \infty$, $A^+ \to 1130K$.

proaches a maximum for the limiting velocity profile, but is everywhere significantly below the experimental value. Neutral stability curves for some of these marginally stable profiles are shown in figure 17.

These calculations strongly indicate that the conjectures that the turbulent velocity profile has unstable or marginally stable eigenvalues were incorrect. Careful examination of the actual content of Malkus's manipulations yields the

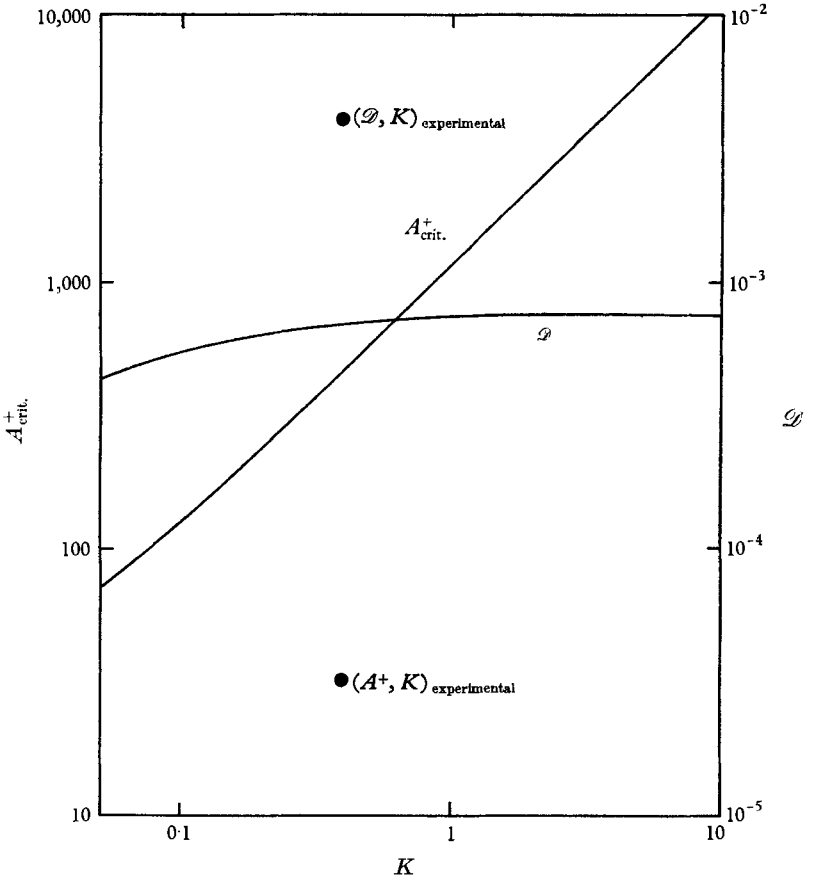

FIGURE 16. Parameters yielding neutrally stable profiles.

explanation for the success of his calculations. Malkus used an approximate characteristic equation for the critical Reynolds number essentially identical with (3.22*b*). The smallest scale λ_0 is tied to the rapid fluctuation of the eigenfunction in the region very close to the wall, and an estimate of c is essentially provided by $c \approx U'_w \lambda_0$. Hence, the determination of $R_{crit.}$ for a specific smallest scale is essentially reduced to an estimation of α. In his calculations Malkus used an estimate of α above which the flow is stable; this estimate was obtained from consideration of positive definite integrals, and is hence conservative. His estimate was

$$8\alpha^4 M > [U'_w R]^2 \quad \text{for stability,}$$

where M is a positive lower bound in excess of 8. Applying this to our experi-

mental profile for $K = 0{\cdot}4$, $A^+ = 31$, $U_c' \approx U_w' = 51{\cdot}5$, we find $\alpha > 2{\cdot}5\,R^{\frac{1}{2}}$. At $R = 25{,}000$ the sufficiency criteria says that the flow will be stable if $\alpha > 395$ (indeed, our neutral stability curve lies below this point). Malkus used this as the estimate for α at the critical point. Upon comparison with the curves of figure 14, we see that it is high by a factor of about 10, and hence his estimate of the critical Reynolds number would be low by about a factor of 10. Thus, in his calculations the profile would indeed appear to be marginally stable, while a more accurate stability calculation indicates it is not. It consequently seems that it was fortuitous that Malkus's calculations met with such apparent success.

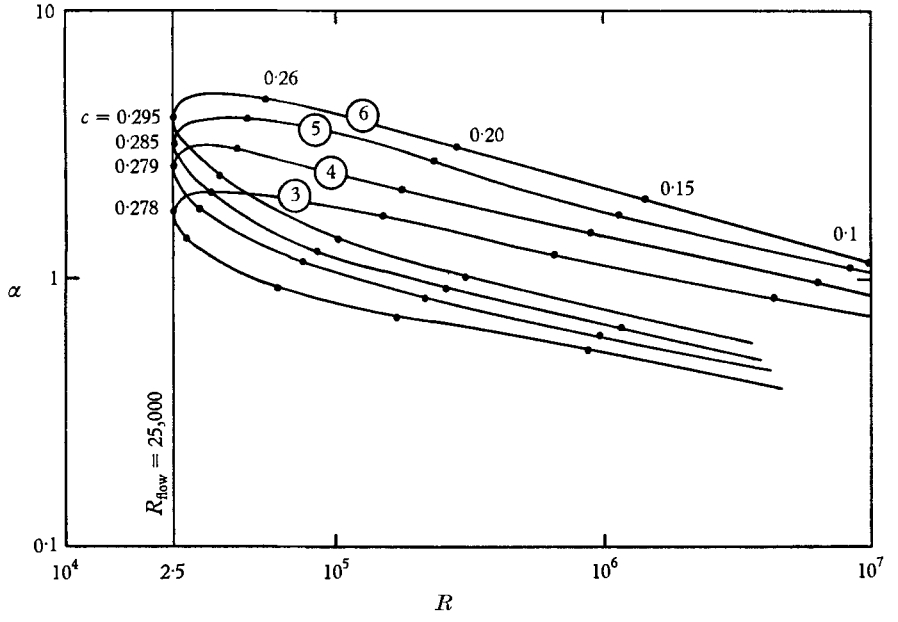

FIGURE 17. Neutral stability curves for marginally stable members of the admissible family. 3, $K = 0{\cdot}05$, $A^+ = 78$; 4, $K = 0{\cdot}10$, $A^+ = 137$; 5, $K = 0{\cdot}20$, $A^+ = 252$; 6, $K = \infty$, $A^+ = 1130K$.

Finally, let us consider the role which the Reynolds stresses would play in the stability problem were they included. The present calculations indicate that the critical point y_c lies within the 'sublayer' for the calculations at hand (at $y^+ \approx 5$ in all cases), where the eddy viscosity is negligible in comparison with the molecular viscosity. Hence the effect of the eddy viscosity on the viscous solutions would have been very small, had it been included. Moreover, consideration of the asymptotic development of the viscous solutions with an eddy viscosity acting indicates that, to first order, ϕ_3 and ϕ_4 would be as given above, except that the Reynolds number would be based on the total viscosity (Tiederman & Reynolds 1965). Hence the neutral stability curve of figure 14 would apply to such a modified Reynolds number, and the neutral curve for R based on the molecular viscosity would be displaced to the right. Thus we conclude that the Reynolds stresses would indeed act to further stabilize the mean profile.

The support of this work by the National Science Foundation and the Air Force Office of Scientific Research is sincerely acknowledged.

REFERENCES

CESS, R. D. 1958 A survey of the literature on heat transfer in turbulent tube flow. *Westinghouse Research Rep.* no. 8–0529–R24.

GAGE, D. H., SCHIFFER, M., KLINE, S. J. & REYNOLDS, W. C. 1966 The non-existence of a general thermokinetic variational principle. *Non-equilibrium Thermodynamics* (eds. Donnelly, R. J., HERMAN, R. & PRIGOGINE, I.). Chicago: University Press.

HOWARD, L. N. 1964 The number of unstable modes in hydrodynamic stability problems. *J. Mecanique,* **3**, 433–43.

LANDAHL, M. 1965 A waveguide model for turbulent shear flow. *NASA* CR-317.

LAUFER, J. 1951 Investigation of turbulent flow in a two-dimensional channel. *NACA Rep.* no. 1053.

LEE, L. H. & REYNOLDS, W. C. 1964 A variational method for investigating the stability of parallel flows. *Tech. Rep.* no. FM-1, *Department of Mechanical Engineering, Stanford University.* Stanford, California.

LIN, C. C. 1955 *The Theory of Hydrodynamic Stability.* Oxford University Press.

LUMLEY, J. 1966 The structure of inhomogeneous turbulent flows. *Proc. International Colloq. on the Fine Scale Structure of the Atmosphere and its Influence on Radio Wave Propagation,* Moscow, June 1965, Dokl. Akad. Nauk (U.S.S.R.).

MALKUS, W. V. R. 1956 Outline of a theory of turbulent shear flow. *J. Fluid Mech.* **1**, 521.

MILES, J. W. 1960 The hydrodynamic stability of a thin film of liquid in uniform shearing motion. *J. Fluid Mech.* **8**, 593.

REYNOLDS, W. C. 1965 *Thermodynamics.* New York: McGraw-Hill.

SPARROW, E. M. & SIEGEL, R. 1959 A variational method for fully developed laminar heat transfer in ducts. *TASME, Series C, J. Heat Transfer,* p. 157.

SPIEGEL, E. A. 1962 On the Malkus theory of turbulence. *Mecanique de la Turbulence,* Paris: Centre National de la Recherche Scientifique, p. 182.

TIEDERMAN, W. G. & REYNOLDS, W. C. 1965 Stability of turbulent Poiseuille flow with application to the Malkus theory of turbulence. *Tech. Rep.* no. FM-2, *Department of Mechanical Engineering, Stanford University.* Stanford, California.

TOWNSEND, A. A. 1962 Remarks on the Malkus theory of turbulent flow. *Mecanique de la Turbulence,* p. 167. Paris: Centre National de la Recherche Scientifique.